# The role of backstress in phase transforming steels

F. D. FISCHER (*) [1], T. ANTRETTER (*),

F. AZZOUZ (**), G. CAILLETAUD (**), A. PINEAU (**),

K. TANAKA (***), K. NAGAYAMA (***)

(*) *Institute of Mechanics, Montanuniversität Leoben,*
*Franz-Josef-Straße 18, A-8700 Leoben, Austria*

(**) *Ecole des Mines, Centre des Matériaux,*
*BP 87, F-91003 Evry Cedex, France*

(***) *Department of Aerospace Engineering,*
*Tokyo Metropolitan Institute of Technology,*
*Asahigaoka 6-6, J-191 Hino/Tokyo, Japan*

TRANSFORMATION INDUCED PLASTICITY (TRIP) is demonstrated by an experimental programme for a Fe-9Ni-12Cr steel for various loading paths with partial or full unloading. The martensitic transformation is considered. A thermodynamical interpretation as well as micromechanical modelling of TRIP are presented. The selection of distinct variants is explained. Finally a modified constitutive equation for the TRIP strain rate is suggested by introducing a transformation surface including a transformation backstress. The backflow after unloading, which cannot be explained by the currently used TRIP strain rate term, can be represented by the proposed formulation. Aspects of future research are discussed.

## 1. Introduction

TRANSFORMATION INDUCED PLASTICITY (TRIP) is now a well-known phenomenon that appears when a material like steel or a shape memory alloy (SMA) transforms, e.g. during a cooling process, and the material is subjected to a certain load-stress. In the "classical" definition we are dealing with the *significantly*

---

[1] Corresponding author

*increased plasticity during a phase change.* Plastic deformation occurs for an externally applied load-stress, even for a load-stress level which is small compared to the yield stress of the parent phase. This is a practical, not a rigorous definition of the "TRIP phenomenon". TRIP is now more widely defined as a coupled phenomenon between transformations and deformations which are not only restricted to plasticity. For further details the reader is referred to the book by Berveiller and Fischer [1] and a review paper by Fischer, Sun and Tanaka [2].

We concentrate here on steels, i.e. materials with the ability to reduce their internal (or free) energy by plastic sliding. Furthermore, we look at the martensitic transformation. Before going into detail, we repeat some aspects of the continuum mechanical representation of the TRIP phenomenon, for details we refer again to [1, 2] and make reference to the papers by Leblond *et al.* [3, 4]. Theses papers are most frequently cited in the context of TRIP.

Usually a linear decomposition of the strain rate contributions is assumed as

$$(1.1) \qquad \dot{\varepsilon}_{ij} = \dot{\varepsilon}_{ij}^e + \dot{\varepsilon}_{ij}^\theta + \dot{\varepsilon}_{ij}^P + \dot{\varepsilon}_{ij}^{TP} + \frac{\delta}{3}\dot{\xi}\delta_{ij}.$$

$\dot{\varepsilon}_{ij}^e$ is the elastic strain rate tensor, $\dot{\varepsilon}_{ij}^\theta$ is the temperature eigenstrain rate tensor, $\dot{\varepsilon}_{ij}^P$ is the plastic strain rate tensor at a fixed volume fraction $\xi$, $0 \le \xi \le 1$, of the product phase (martensite), $\dot{\varepsilon}_{ij}^{TP}$ is the TRIP strain rate tensor and $\frac{\delta}{3}\dot{\xi}\delta_{ij}$, with the unity tensor $\delta_{ij}$, may be considered as the metallurgical strain rate tensor, where $\delta$ stands for the volume change due to the phase transformation. A dot $(\cdot)$ represents the total material derivative. The TRIP strain rate tensor according to Leblond's proposal is given by

$$(1.2) \qquad \dot{\varepsilon}_{ij}^{TP} = \frac{3}{2}K\frac{d\varphi}{d\xi}\dot{\xi}S_{ij}.$$

$\varphi(\xi)$ is a – more or less – heuristic function of $\xi$, e.g.

$$(1.3) \qquad \varphi(\xi) = \xi(2 - \xi),$$

$K$ is the TRIP constant and $S_{ij}$ is the global stress deviator associated to the stress tensor $\sigma_{ij}$ which can be assumed as the average over a representative amount of grains (remark: several authors consider to be the stress deviator at the "mesoscopic" level). The TRIP constant $K$ is assumed to be a function of $\delta$ being of the order of $5.0*10^{-5}$ MPa$^{-1}$.

The concept as outlined above is implemented in several programs like Sysweld [5] and applied with more or less success for quenching (heat treatment) applications. However, experiments by the group of Cailletaud and

PINEAU, (see e.g. [6, 7]), have shown that the proposal (1.2) does no longer hold true if a non-monotonic loading path (e.g. a full or partial unloading) is followed. Even if a compression test is performed, the constant K must be modified. Therefore, the group of authors of this paper have been performing, for some years now, an extensive experimental programme on the TRIP effect for multiaxial loading and non-monotonic loading paths. This experimental work forms the basis for a better understanding of the TRIP effect as well as for the improved formulation of a TRIP strain rate.

Two crucial phenomena are discussed in the present paper:

- First, the orientation effect (Magee effect) in the martensitic transformations: Martensite variants with different orientations, are formed even during full or partial unloading, resulting in a further TRIP strain growth. The change in the internal stresses around the martensite variants is an important factor to be considered.

- Second, the backstress which, according to the present experiments, must be included in the constitutive equation for the TRIP strain. The evolution of the backstress is also an issue to be investigated.

## 2. Experimental programme

The test material used was a Cr-Ni-Mo-Al-Ti Maraging steel, provided by Aubert and Duval, first introduced for TRIP testing by CAILLETAUD et PINEAU et al. – see [6, 7] – and referred to as Marval X12. The martensite start temperature Ms is found at ca. 150° (423 K), the martensite finish temperature $M_f$ at ca. 80° (353 K). This material is ideally suited for TRIP tests since it transforms to martensite even upon cooling in air. The quenching capability is excellent, leading to no corrosion or oxidation. All these properties allow to use the same specimen several times. For the sake of completeness, the nominal composition is given in Table 1.

Table 1. Nominal composition of the investigated material (weight percent), rest Fe

| Cr | Ni | Mo | Al | Ti | C | Si | Mn | P | S | N |
|-------|------|------|------|------|--------|------|------|-------|---------|--------|
| 12.15 | 9.05 | 2.03 | 0.70 | 0.35 | < 0.01 | 0.05 | 0.03 | 0.009 | < 0.002 | 0.0045 |

Tubular specimens were machined with a mid-circle radius of 9 mm and a wall thickness of 1.5 mm. The specimens were machined out of rods with an average diameter of 30 mm. Then the specimen is cooled down to the temperature of

200° C (473 K) and the load is applied. Both tension or compression and shear loading are possible. To understand the influence of the microstructure, full or partial unloading is performed at a certain volume fraction $\xi$ of martensite. All the experiments have been performed in the Laboratory of Prof. K. Tanaka. Due to space restrictions, further important information on the material is given without any detail:

Figure 1 demonstrates the stress-strain curve at 205° C (478 K) (full austenite) and at room temperature 30° C (303 K), (full martensite). As can be seen, the material shows a rather soft austenitic and a surprisingly strong martensitic phase.
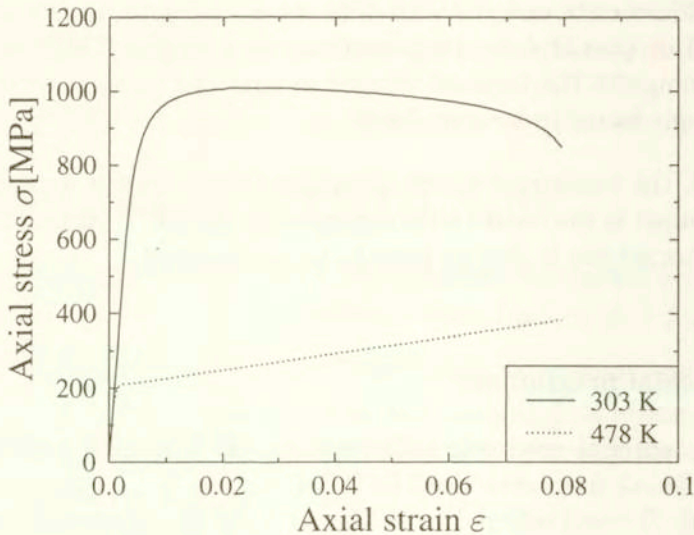


FIG. 1. Stress ($\sigma$)-strain ($\varepsilon$)-curve at 30° C (303 K) (full martensite) and at 205° C (478 K) (full austenite).

The following data can be given for the thermoelastic constants:

- Young's modulus E $\sim$ 205.000 MPa at room temperature,
  $\sim$ 179.000 MPa at 180° C (453 K).

- The average value of Poisson's ratio $\nu = 0.33$.

- Average values for the integral thermal expansion coefficients in the temperature range up to 200° C (473 K) are

$$\alpha_\gamma = 19.6 \times 10^{-6} {}^\circ\,C^{-1}, \quad \alpha_\alpha = 11.37 \times 10^{-6} {}^\circ\,C^{-1}.$$

– Application of the crystallographic theory of martensite with the measured lattice constants of both phases yields the transformation volume change $\delta_c$ and the transformation shear $\gamma_c$. The subscript "c" indicates that these values have been calculated analytically,

$$\delta_c = 0.0178, \quad \gamma_c = 0.227.$$

– A common way to measure $\delta$ is to perform a dilatometer test. Those tests were run both for the tubular specimens, called "longitudinal specimens" with respect to the position of the original rod they were machined from, and for very tiny specimens (diameter 2 mm, length 12 mm) in various directions, including radial, relative to the axis of the original rod. Figure 2 shows an "open" loop for the "longitudinal" specimen without any load-stress and an almost perfectly closed dilatation loop for an equal specimen obtained with a hold stress of $\sigma_h = 28$ MPa. Closer inspection of the tiny specimens reveals that the total transformation volume change seems to split in an anisotropic way into $\delta/3 - \delta_a = \tilde{\delta}/3$ in the longitudinal direction, and $\delta/3 + \delta_a/2$ in the radial and circumferential direction. Finally, the dilatometer tests yield $\delta_a = 0.0016$ and $\delta = 0.0192$. Although these values differ somewhat from $\delta_c$, they are used for further investigations since they stem from direct experimental observation and are understood as the result of the internal stresses.
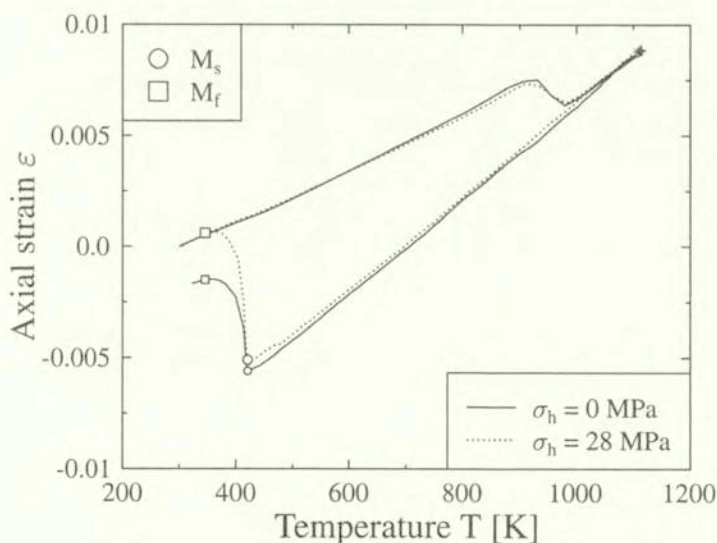


FIG. 2. Dilatometer test for a longitudinal specimen, load-stress-free and with load-stress $\sigma_h = 28$ MPa.

Dilatometer tests are usually applied to determine the transformed volume fraction $\xi$ in accordance with the actual volume change. The following transformation kinetics can be found:

$$(2.1) \quad \xi = 1 - \exp[-0.0549(M_\sigma - T)], \quad M_\sigma = M_s + 0.046\sigma \quad \text{in MPa;}$$

the label "$\sigma$" in this case represents the tension load-stress on the specimen.

As a first result, the $M_\sigma$ (Martensite start) and $M_f$ (Martensite finish) lines are shown in Fig. 3. They are generated from dilatometer curves performed by the tubular specimens for various hold stresses. One can see clearly that the slope of the start line depends on the kind of loading, as explained in the next section. Obviously a shift of the $\sigma$-reference line to $X_z = 28$ MPa leads to the known picture of a $M_\sigma$-line. The stress component $X_z$ can, therefore, at first be interpreted as an initial backstress. The former results combined with the yield stress of the material is depicted in Fig. 4. It is vital to mention here that the off-set strain (0.05% or 0.005%) plays a significant role with respect to the definition of the yield stress. The large difference in $\sigma_{0.05}$ and $\sigma_{0.005}$ in the low temperature range can be attributed to the higher work-hardening than in the high temperature range. Actually in this temperature range the specimen is composed of the thermally and stress-induced martensite phase which is much harder than the soft parent phase. The "hook-type" tendency on the left side of the $M_\sigma$-line points to this "composite"-effect and would give rise to a rather extensive discussion on its own, and will be published elsewhere. Figure 5 shows
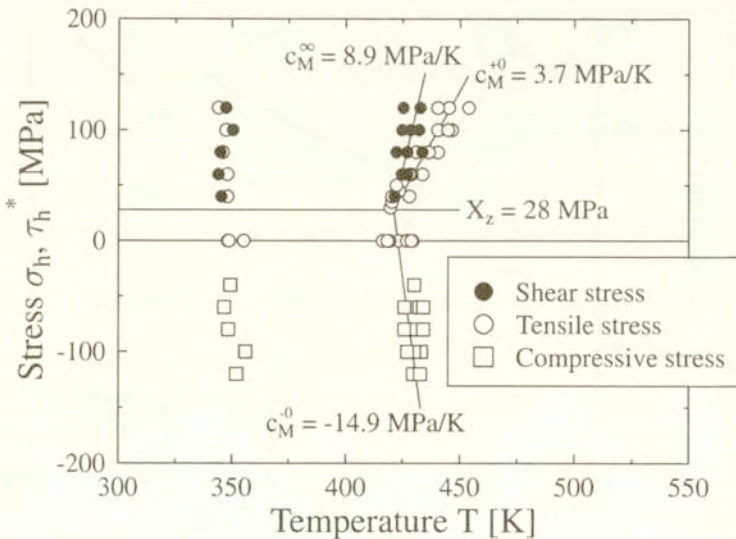


Fig. 3. $M_\sigma$-lines (slope $c_M^{+0}$ for tension, $c_M^{-0}$ for compression, $c_M^\infty$ for shear) and $M_f$ lines.

the TRIP strain $\varepsilon^{TP}$ for various tensile hold stresses and partial or full unloading, calculated from the relation (2.2).
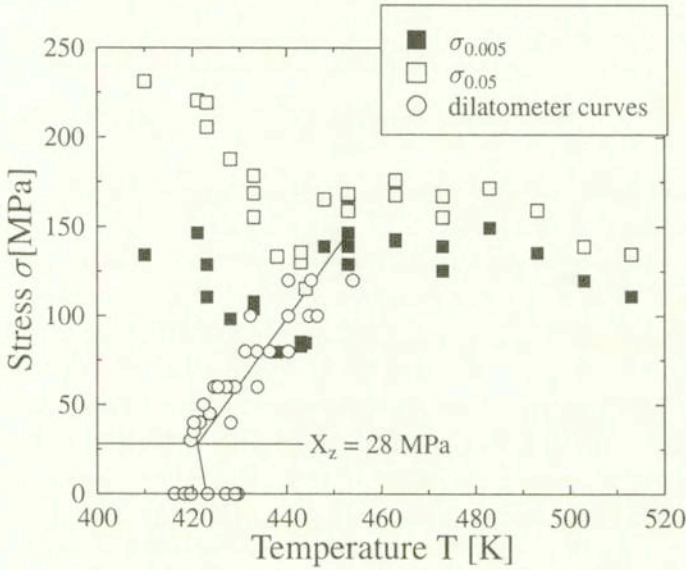


FIG. 4. Combined yield and transformation behaviour characterising the MARVAL X12 steel.
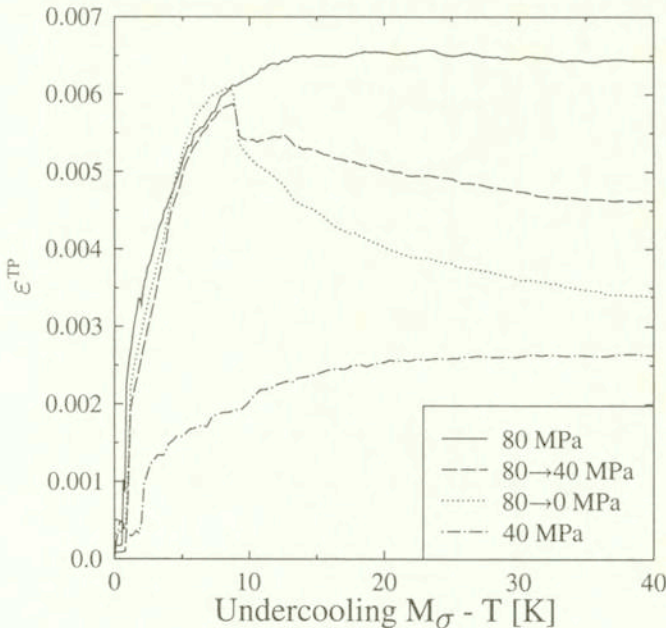


FIG. 5. TRIP-strain $\varepsilon^{TP}$ versus the undercooling temperature difference $(M_\sigma - T)$-curves for tension tests; $80 \to 0$ MPa, $80 \to 40$ MPa means unloading from 80 MPa to 0 MPa or 40 MPa, respectively.

$$(2.2) \qquad \varepsilon^{\mathrm{TP}}\Big|_{M_\sigma - T} = \varepsilon\Big|_{M_\sigma - T} - \varepsilon\Big|_{M_\sigma} - \frac{\tilde{\delta}}{3}\xi - (M_\sigma - T)[\alpha_\alpha \xi + \alpha_\gamma(1 - \xi)];$$

$\varepsilon^{\mathrm{TP}}\big|_{M_\sigma - T}$ represents the TRIP-strain to a temperature difference $(M_\sigma - T)$, (calculated);

$\varepsilon|_{M_\sigma - T}$ stands for the total strain to a temperature difference $(M_\sigma - T)$, (measured);

$\varepsilon|_{M_\sigma}$ is the total strain at the temperature $M_\sigma$, (measured).

The data applied in (2.2) have been provided above.

Tests were carried out as follows: In the process of cooling with a rate of 2 K/s, after annealing and austenitization at 840° C for 30 min, a stress $\sigma_h = 80$ MPa is applied at 200° C with the loading rate 80 MPa/s and held constant in the subsequent process. The subscript "h" to $\sigma$ and later $\tau^*$ will refer to the fact that the load is held constant for a certain period of time. The hold stress is then unloaded partially (to 40 MPa) or fully (to 0 MPa) with the unloading rate of 80 MPa/s at a temperature ca. 10° C lower than $M_\sigma$. The total strain is measured during the entire thermomechanical loading process. As already mentioned, a TRIP strain of $-0.016$ occurs without any load. No TRIP strain appears at a hold stress of 28 MPa as shown in Fig. 2. This induces a certain asymmetry
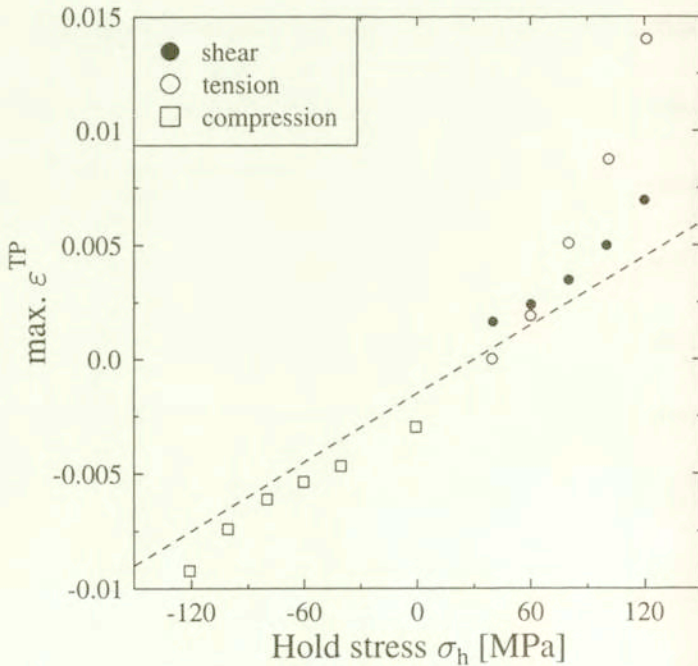


Fig. 6. The "Greenwood-Johnson" line $K = 5 \times 10^{-5}$ MPa$^{-1}$ in relation to the maximum TRIP strain for several hold stress levels.

with respect to tension and compression. Obviously an internal stress $X_z$ state is active, a backstress, which leads to a reduced hardening in the tension regime and, therefore, to higher TRIP strain compared to the compression regime.

As mentioned in the introduction, Greenwood and Johnson proposed a linear relation between the maximum TRIP strain and the hold stress. A line with the slope $K = 5.0 \cdot 10^{-5}$ MPa$^{-1}$ is plotted in Fig. 6 with its origin at $X_z = 28$ MPa. The plots show the results of the tests under constant hold stress. The deviation from this straight line clearly demonstrates the strong sensitivity to $\sigma_h$ in the tension regime. An interesting fact that will be explained qualitatively in the next section is that the maximum TRIP strain is less sensitive to the hold stress in shear tests. The following two figures demonstrate the TRIP strain for a specimen under compression (Fig. 7) and under shear (Fig. 8), subjected to a hold stress of 80 MPa with constant loading, partial unloading from 80 MPa to 40 MPa and full unloading. To compare the shear tests with the tension tests, an equivalent stress $\tau^* = \tau\sqrt{3}$ and an equivalent strain $\gamma^* = \gamma/\sqrt{3}$ are introduced.



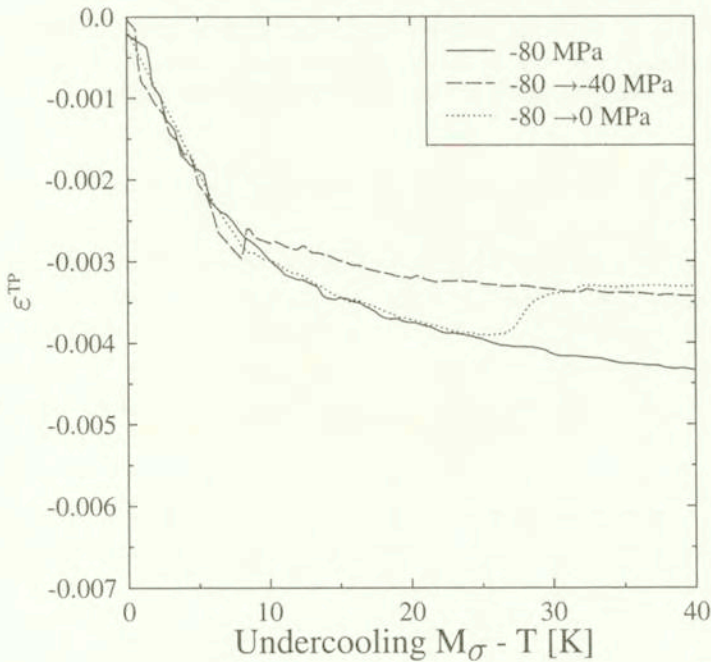FIG. 7. TRIP-strain $\varepsilon^{\mathrm{TP}}$ versus the undercooling temperature difference $(M_\sigma - T)$-curves for compression tests; $80 \rightarrow 0$ MPa, $80 \rightarrow 40$ MPa, means unloading from 80 MPa to 0 MPa or 40 MPa, respectively.
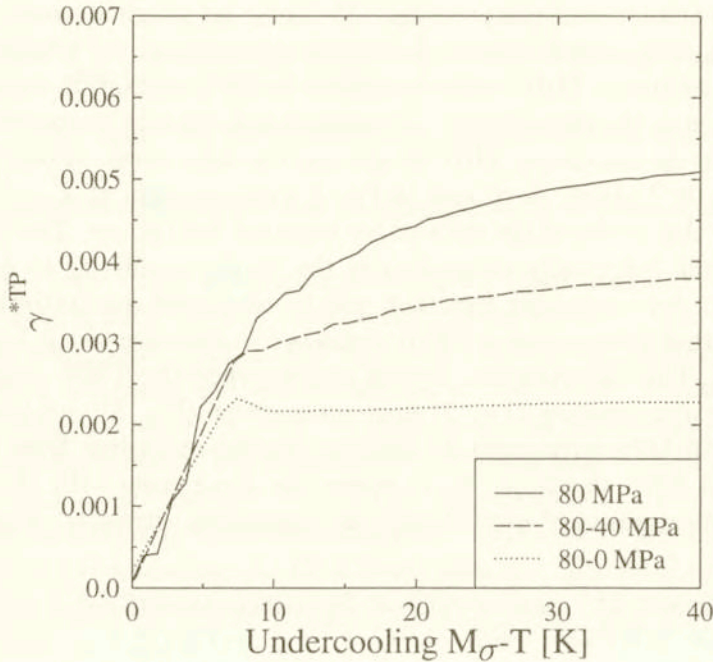
Fig. 8.   TRIP-strain $\gamma^{*TP}$ versus the undercooling temperature difference $(M_\sigma - T)$ -curves for shear tests; $80 \to 0$ MPa, $80 \to 40$ MPa means unloading from $\tau^* = 80$ MPa to $\tau^* = 0$ MPa or $\tau^* = 40$ MPa, respectively.

In the case of full unloading (and to a certain degree also with partial unloading) one can observe a significant "backflow" in the tension regime, (see Fig. 5). The "backflow" is smaller but still clearly observable in the compression regime, (see Fig. 7). Since after unloading only the internal stress state influences the formation of martensitic variants, the formation of some new variants obviously reduces the absolute length of the specimen, although the specimen is totally unloaded. The total stress state before unloading (that means the load-stress state plus the internal stress state) obviously leads to an arrangement of martensitic variants that contributes to the "orientation" effect of the TRIP strain. After unloading, some further variants develop which "compensate" the orientation effect to a certain degree. A thermodynamical interpretation is given in the next chapter. The situation is obviously different in the case of shear loading and the TRIP shear strain $\gamma^{*TP} = \gamma/\sqrt{3}$, (see Fig. 8). In fact, the TRIP shear strain of the specimen remains nearly unchanged after unloading. Obviously the internal stress state after shear unloading is not apt to favour some martensitic variants which contribute to an irreversible shear strain.

The conclusion is that a relation of the type (1.2) cannot be applied to an unloading process in the case of tensile or compressive loading, since $S_{ij} = 0$ would

entail $\dot{\varepsilon}_{ij}^{\mathrm{TP}} = 0$, which contradicts the experimental evidence. However, in the case of shear loading, Eq. (1.2) obviously remains applicable. As a consequence, the authors suggest to reflect both the initial backstress (i.e. $X_z$ in the uniaxial case) and the backstress contribution due to "backflow" by a transformation backstress tensor $X_{ij}^{\mathrm{TP}}$ in order to establish a more realistic constitutive law for phase transforming materials.

## 3. Transformation thermodynamics

### 3.1. Transformation condition

As mentioned above, the martensitic transformation is accompanied by a transformation volume change $\delta$ and a transformation shear $\gamma$, finally leading to a transformation tensor $\varepsilon_{ij}^*$ with the non-zero components $\varepsilon_{13}^{**} = \varepsilon_{31}^* = \gamma/2$, $\varepsilon_{33}^* = \delta$, described in a local coordinate system with respect to the habit plane of a variant. Both their values as well as the orientation of the martensitic variants (in general 24) can be found by applying the mathematical (crystallographic) theory of martensite. The reader is referred here to the pioneering work by Wechsler, Lieberman and Read (1953), for details see the paper by MARKETZ *et al.* [8]. The orientation of the variants is described by the set of 3 Eulerian angles. The understanding of the effect of a stress state on the formation of a specific martensitic variant goes back to an equally pioneering work by Patel and Cohen (1953). The role of the stress state was intensively studied with respect to the microstructure and the global stress-strain behaviour of shape memory alloys (SMAs). Recently a transformation condition for a microregion $V_\mu$ was presented by LEVITAS, (see e.g. [9]) and FISCHER *et al.* [10]. This condition reads

$$(3.1) \qquad \int_{V_\eta} \sigma_{ij}\,|_{t_s} \varepsilon_{ij}^* dV + V_\mu [\![\rho\varphi_{\mathrm{chem}}]\!] \geq V_\mu F_c + \Delta\Gamma + W_{p\ell}^\tau + W_{e\ell}^\tau.$$

$\sigma_{ij}|_{t_s}$ represents the stress state just at the onset of transformation. $[\![\rho\varphi_{\mathrm{chem}}]\!]$ is the difference of the chemical free energy of the stress-free parent phase and the product (martensite) phase. $F_c$ is a transformation barrier representing the energy necessary for rearranging the crystallographic lattice (– a given entity which must be measured). $\Delta\Gamma$ represents the surface energy produced during the formation of $V_\mu$ and is usually small in the case of plate-type microstructures. $W_{p\ell}^\tau$ and $W_{e\ell}^\tau$ are the additional plastic and elastic work terms, resp., only due to the stress fluctuation $\tau_{ij}$ during the transformation process. REISNER *et al.* give values for these quantities in [11]. As one can easily see, the left-hand side contains a mechanical and a chemical driving force. The transformation condition

is now applied to interpret both the varying slope of the martensite start line and the development of the TRIP strain.

### 3.2. Slope of the martensite start line

Figure 3 shows clearly that the martensite start line shows a different slope $c_M$ depending on the loading case. Since, to the best knowledge of the authors, such an observation has not been reported for steels yet, an interpretation is presented. A study assuming equal chemical energies for various loading conditions allows to compare the influence of distinct load cases represented by $\Sigma_{ij}$ on the mechanical driving force (MDF), with

$$(3.2) \qquad \qquad \text{MDF} = \Sigma_{ij}\varepsilon_{ij}^*.$$

This was done by Marketz et al. [8] allowing the full space of Eulerian angles to describe a possible martensitic variant (– which is reasonable in a polycrystal). Consideration of a global coordinate system and principal stresses $\Sigma_{11}$, $\Sigma_{22}$, $\Sigma_{33}$ the MDF yields

$$(3.3) \qquad \text{MDF} = \Sigma_{33}\frac{1}{2}\left(\delta + \sqrt{\delta^2 + \gamma^2}\right) + \Sigma_{11}\frac{1}{2}\left(\delta - \sqrt{\delta^2 + \gamma^2}\right)$$

$$\text{for} \quad \Sigma_{33} > \Sigma_{22} > \Sigma_{11}.$$

We now compare three loading cases with the same equivalent stress $\tau_T$ according to Tresca, $\tau_T = \dfrac{1}{2}(\Sigma_{33} - \Sigma_{11})$, leading to

$$(3.4) \qquad \text{MDF} = (\Sigma_{33} + \Sigma_{11})\delta/2 + \tau_T\sqrt{\delta^2 + \gamma^2} :$$

– a tension state $\Sigma_{33} > 0, \Sigma_{11} = 0, \tau_T = \Sigma_{33}/2,$

$$(3.5) \qquad \text{MDF}_T = \tau_T\frac{\delta}{2} + \tau_T\sqrt{\delta^2 + \gamma^2};$$

– a compression state $\Sigma_{33} = 0, \Sigma_{11} < 0, \tau_T = -\Sigma_{11}/2,$

$$\text{MDF}_c = -\tau_T\frac{\delta}{2} + \tau_T\sqrt{\delta^2 + \gamma^2};$$

– a shear state $\Sigma_{33} = -\Sigma_{11}, \tau_T = \Sigma_{33},$

$$(3.6) \qquad \text{MDF}_s = \tau_T\sqrt{\delta^2 + \gamma^2}.$$

Assuming the same value of $\tau_T$ tension produces the highest amount of MDF and shows the strongest influence on the martensite start line (see Fig. 3, $c_M = 3.7$ MPa/K). The shear state produces the intermediate value of MDF. The lowest

value of MDF is found for the compression state. Figure 3 indicates that the slope of the shear martensite start line ($c_M = 8.9$ MPa/K) is more affected by the stress state than the compression martensite start line ($c_M = -14.9$ MPa/K), which exhibits the steepest slope.

This study indicates that the selection of martensitic variants is not only influenced by the magnitude of the stress state (characterised by the equivalent stress) but also by the "orientation relation" between the considered martensitic variant and the stress state.

### 3.3. Mechanisms for the TRIP strain

The formation of the transformation strain itself and the selection of locally optimal variants are responsible for the irreversible deformation of an iron-based alloy during and after martensitic phase transformation, and lead to the following two mechanisms:

– The accommodation process due to $\delta$ and $\gamma$ enforcing additional elastic and plastic straining in relation to the load-stress state, eventually producing a compatible deformation (and strain) state. This process is often called the "Greenwood-Johnson" effect or "plastification" effect.

– The orientation process due to the formation of preferred variants which may be arranged in some (partially) "self-accommodating" groups. This effect is often referred to as "Magee" or "orientation" effect.

Some further comments may be important:

– There is nowadays a clear evidence that SMAs "thrive" only on the orientation effect, that means through the formation of selected variants. The global deformation state depends on the overall elastic strain and the average transformation tensor

$$(3.7) \qquad \varepsilon_{ij}^{\mathrm{TP}} = \frac{1}{V} \int\limits_{V} \varepsilon_{ij}^{*} dV.$$

SMAs show nearly no volume change and no plastic straining up to a significant stress level. Their original shape can be restored e.g. by heating.

– The orientation effect in steel was recognized only very recently, e.g. in the work of the "Nancy" group, (see e.g. [12, 13]). Most recent experimental observations which have not been published yet, explain the back-transformation in the temperature range of 900 K to 1000 K also, at least partially, as a displacive (martensite-type) transformation. The retained martensite is then transformed at temperatures above this range by a diffusive process. At temperatures lower than ca. 900 K, obviously the martensite variants are pinned by dislocations produced mainly by the accommodation of the volume change. There is a clear

evidence that such high temperatures are necessary to provide the dislocations with enough mobility to release the martensite variants.

### 3.4. Modelling of the backstress due to "backflow"

Micromechanical modelling has been applied to shed more light on the developing microstructure, both for a loaded and later (partially) unloaded specimen.
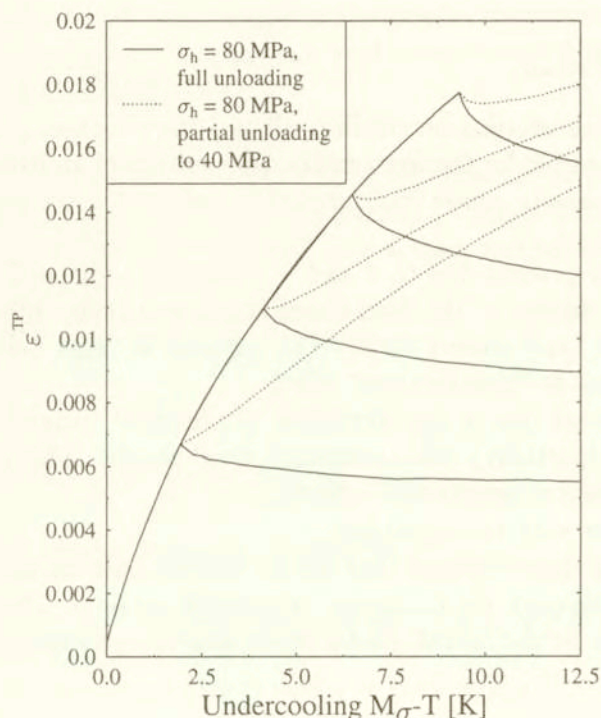


FIG. 9. Simulated TRIP strain $\varepsilon^{TP}$ versus to the undercooling temperature difference $(M_\sigma - T)$. The hold stress $\sigma_h = 80$ MPa. Full lines represent unloading to 0 MPa, dotted lines to 40 MPa.

FISCHER et al. [14] presented an extensive report on micromechanical modelling of the TRIP effect for specimens subjected to tension or compression, with a full or partial unloading after a certain volume fraction of martensite. They applied the numerical realisation of the transformation condition (3.1) according to a concept by REISNER [15]. Specifically, the backflow due to unloading (see Fig. 5 for tension and unloading and Fig. 7 for compression and unloading) has to be investigated by a numerical method. Only two figures are repeated from this study. Figure 9 shows the TRIP strain depending on the undercooling temperature difference $(M_\sigma - T)$. Note that $(M_\sigma - T)$ is related to $\xi$ by (2.1). Full or

partial unloading from the originally constant stress state of 80 MPa is simulated. Obviously the micromechanical study yields a certain backflow after full unloading. Figure 10 supplies a statistical evaluation of the number of variants which have developed during the progress of transformation. At the initial step of the transformation, the favourite variant in a grain of a polycrystal is created. With the ongoing transformation, an eigenstress state is generated which leads to an increasing number of different variants. Obviously those variants develop which arrange in such a way that a certain "self-accommodation" of the transformation shear can be observed. After the partial unloading, two to three further variants become now favourably oriented due to the residual stress state. This effect is of course more pronounced in the case of full unloading. These new variants enforce a reduction of the length of the specimen by an additional "self-accommodation" to variants developed earlier. The study shows furthermore that after full unloading no further plastification occurs, and that the change in shape is solely due to the "orientation"-effect.
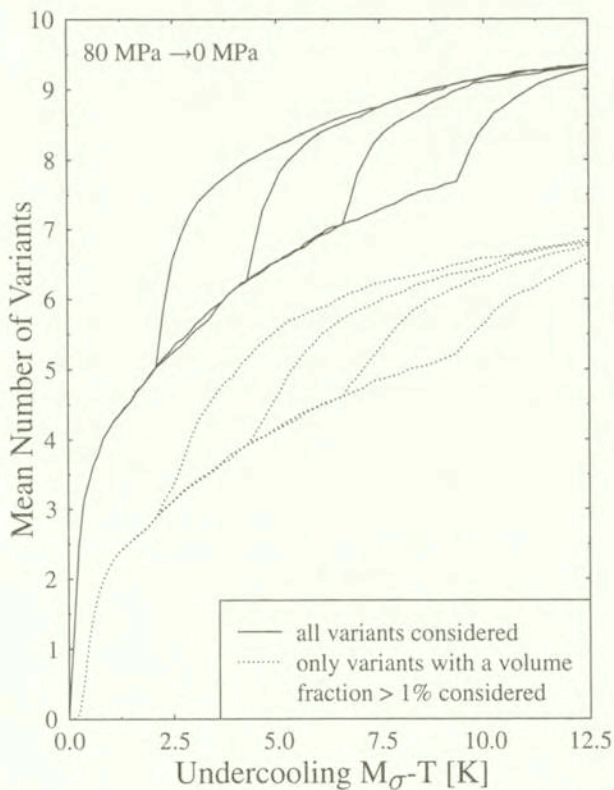


FIG. 10. Number of variants for partial unloading from 80 MPa. The full lines represent all variants, the dotted lines those with a volume contribution of more than 1%.

## 4. A Hypothetical transformation surface

As explained in the Introduction, we assume a linear decomposition of the strain rate tensor. Furthermore, we introduce a hypothetical transformation surface (assuming the usual summation convention over repeated indices) as

$$(4.1) \qquad f^{\mathrm{TP}} = \left(1 - \tilde{\beta}\right) J_2 \left(\sigma_{ij} - X_{ij}^{\mathrm{TP}}\right) + \tilde{\beta} \left(J_1 \left(\sigma_{ij} - X_{ij}^{\mathrm{TP}}\right)\right)^2$$

$$+ \tilde{\gamma} J_1 \left(\sigma_{ij} - X_{ij}^{\mathrm{TP}}\right) - \left(R^{\mathrm{TP}}\right)^2$$

with $\tilde{\beta}$, $\tilde{\gamma}$ and being the fit parameters and $R^{\mathrm{TP}}$ affecting the size of the surface. This surface includes the transformation backstress $X_{ij}^{\mathrm{TP}}$.

$J_1$, $J_2$ are the two invariants of the reduced stress tensor $\sigma_{ij} - X_{ij}^{\mathrm{TP}}$,

$$(4.2) \qquad J_1 \left(\sigma_{ij} - X_{ij}^{\mathrm{TP}}\right) = \sigma_{ii} - X_{ii}^{\mathrm{TP}},$$

$$(4.3) \qquad J_2 \left(\sigma_{ij} - X_{ij}^{\mathrm{TP}}\right) = \left[\frac{3}{2} \left(S_{ij} - \hat{X}_{ij}^{\mathrm{TP}}\right) : \left(S_{ij} - \hat{X}_{ij}^{\mathrm{TP}}\right)\right].$$

$S_{ij}$ is the deviator of $\sigma_{ij}$, $\hat{X}_{ij}^{\mathrm{TP}}$ is the deviator of $X_{ij}^{\mathrm{TP}}$. Of course, if we assume $X_{ij}^{\mathrm{TP}}$ being a deviator, then

$$(4.4) \qquad\qquad J_1 = \sigma_{ii}.$$

The above hypothetical surface (4.1) includes the value of $J_1$ itself to distinguish between the tension and the compression regime or, in other words, to describe the asymmetry of the transformation domain in tension and compression. If $f^{\mathrm{TP}}$ reaches 0, then the stress state is sufficient to produce a "macroscopic TRIP flow". If $f^{\mathrm{TP}}$ is smaller than 0, then no macroscopic TRIP effect can be observed. The TRIP strain rate will be assumed to be proportional to $\langle f^{\mathrm{TP}} \rangle^{1/2}$, $\langle a \rangle$ is $a$ for $a > 0$ and 0 for $a \leq 0$, defined as

$$(4.5) \qquad\qquad \dot{\varepsilon}_{ij}^{\mathrm{TP}} = \frac{1}{2} K \frac{d\varphi}{d\xi} \dot{\xi} \langle \frac{f^{\mathrm{TP}}}{J_2} \rangle^{1/2} \frac{\partial J_2}{\partial \sigma_{ij}},$$

$$(4.6) \qquad\qquad \frac{\partial J_2}{\partial \sigma_{ij}} = 3 \left(S_{ij} - \hat{X}_{ij}^{\mathrm{TP}}\right).$$

Note that $\dot{\varepsilon}_{ij}^{\mathrm{TP}}$ is now parallel to $\left(S_{ij} - \hat{X}_{ij}^{\mathrm{TP}}\right)$ and not only to $S_{ij}$ as reported in the literature, (see e.g. [1 – 5]). This assumption allows a nonzero TRIP strain rate even for $S_{ij} \equiv 0$, (see also [6])!

We adapt now the transformation surface to the experiments explained in Sec. 2. Let us assume a tension or compression stress $\sigma$ coupled with shear stress $\tau$ and consider a plane stress case (like in the tubular specimens investigated). As reported already, we found a backstress component $X_{11}^{TP} = X_z = 28$ MPa but no backstress component with respect to shear. Direction 1 corresponds to the longitudinal direction. According to the dilatometer test, no backstress is assumed in directions 2 and 3 leading to $\hat{X}_1^{TP} = \hat{X}_z = \dfrac{2}{3}X_z$. $J_1, J_2$, and $f^{TP}$ will now read

$$(4.7) \qquad J_1 = \sigma - X_z,$$

$$(4.8) \qquad J_2 = (\sigma - X_z)^2 + 3\tau^2,$$

$$(4.9) \qquad f^{TP} = (\sigma - X_z)^2 + 3(1 - \tilde{\beta})\tau^2 + \tilde{\gamma}(\sigma - X_z) - (R^{TP})^2.$$
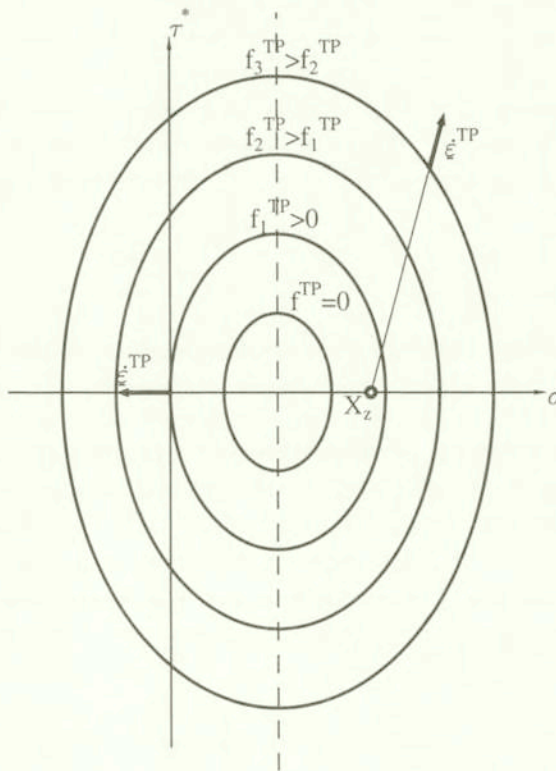


FIG. 11. Isolines for a hypothetical transformation surface for the TRIP strain rate in the modified deviator space $S$, $\tilde{\tau} = (1 - \tilde{\beta})\tau$, $\hat{X}_z = 19$ MPa, $\tilde{\beta} = 0.31$, $\tilde{\gamma} = 44$ MPa; $R^{TP}$ size parameter of the transformation surface.

Working in the $\sigma, \tau^* = \tau\sqrt{3}$ space allows to represent $J_2$ by a circle with the centre at $\sigma = X_z$, $\tau^* = 0$ and the transformation surface by an ellipse with the centre at $\sigma = X_z - \tilde{\gamma}/2$, $\tau^* = 0$ and the semi-axes $e_\sigma$, $e_{\tau^*}$. in the direction, resp.,

$$(4.10) \qquad\qquad e_\sigma = \left((R^{\mathrm{TP}})^2 + \tilde{\gamma}/4\right)^{1/2},$$

$$(4.11) \qquad\qquad e_{\tau^*} = e_\sigma/(1 - \tilde{\beta})^{1/2}.$$

The situation is qualitatively depicted in Fig. 11. Both relevant components of the TRIP strain rate can be assembled to a vector with a radial orientation relative to the $J_2$ surface. The curve $f^{\mathrm{TP}} = 0$ is an ellipse enclosing an area with no further TRIP strain rate. Figure 11 shows schematically the isolines for a transformation surface and some TRIP strain vectors. In the case of $\tau^* = 0$ one can recognize that, firstly, the TRIP strain rates are different for tension and compression for the same load stress intensity and, secondly, that for $\sigma = 0$ (a stress-free specimen, e.g. after unloading) a TRIP strain rate is also possible.

In general, the four parameters describing the transformation surface, $X_z$, $\tilde{\gamma}$, $\tilde{\beta}$, $R^{\mathrm{TP}}$ may evolve with the loading process, since they reflect the microstructure of the material correlating with its transformation behaviour. This requires to develop a proper evolution law. Since a broad experimental basis is a mandatory prerequiste, the proposal for any evolution law can only be the subject of further research. The group of the authors will work in this field in the next years.

## 5. Conclusion

A broad experimental programme is presented for an Fe-Ni-Cr steel, monitoring the TRIP strain for monotonic and non-monotonic loading paths like partial and full unloading. Even in the case of dilatometer tests without any external load, a backstress can be observed. In the case of unloading, a backflow can be observed depending on the kind of preloading. Transformation thermodynamics is employed to show the influence of the load-stress state and the internal stress state on the formation of an irreversible transformation strain. This TRIP strain consists of two contributions, i.e. one due to the plastic accommodation of the transformation eigenstrain and one due to the selection of distinct martensitic variants. The second effect, named "orientation" effect, can clearly be shown even for a very low load level by means of different martensite start lines. The hypothesis of the existence of a significant orientation effect is supported by means of micromechanical modelling.

The TRIP strain rate proposed in the available literature does not account for the existence of a transformation backstress. Inspired by the work of Prof. Z. Mróz introducing additional surfaces to the yield surface in order to

explain the backstress in the case of classical plasticity, we also define a transformation surface in order to determine the backstress in the case of a phase transformation. The TRIP strain rate can be represented by a vector from the origin of the transformation surface to the corresponding stress point on the transformation surface. The amount of the TRIP strain rate is also related to the actual value of the transformation surface function. Finally this concept is intended to contribute to the development of improved constitutive equations for phase changing materials subjected to arbitrary loading paths.

## References

1. M. BERVEILLER and F. D. FISCHER, *Mechanics of solids with phase changes*, Springer Wien, New York 1997.

2. F. D. FISCHER, Q.-P. SUN and K. TANAKA, *Transformation-induced plasticity (TRIP)*, ASME Appl. Mech. Rev. **49**, 317–364, 1996.

3. J. B. LEBLOND, G. MOTTET and J. C. DEVAUX, *A theoretical and numerical approach to the plastic behaviour of steels during phase transformations – I: Derivation of general relations; II: Study of classical plasticity for ideal-plastic phases*, J. Mech. Phys. Solids, **34**, 395–410, 411–432, 1986.

4. J. B. LEBLOND, J. DEVAUX and J. C. DEVAUX, *Mathematical modelling of transformation induced plasticity in steels – I: Case of ideal-plastic phases – II: Coupling with strain hardening phenomena*, Int. J. Plasticity, **5**, 551–572, 573–591, 1989.

5. Sysweld + 2.0: Reference Manual, SYSTUS International, ESI Group: Simulation of Welding and Heat Treatment Processes, Framasoft + CSI, 1997.

6. J.-Chr. VIDEAU, G. CAILLETAUD and A. PINEAU, *Modélisation des effets mécaniques des transformations de phases pour le calcul de structures*, J. de Physique IV, Colloque C3, Supplm. J. de Physique III, **4**, C3-227–C3-232, 1994.

7. J.-Chr. VIDEAU, G. CAILLETAUD and A. PINEAU, *Experimental study of the transformation – induced plasticity in a Cr-Ni-Mo-Al-Ti steel*, J. de Physique IV, Colloque C1, Supplm. J. de Physique III, **6**, C1-465–C1-474, 1996.

8. F. MARKETZ and F. D. FISCHER, *A mesoscale study on the thermodynamic effect of stress on martensitic transformation*, Met. Mater. Trans., **26A**, 267–278, 1995.

9. V. I. LEVITAS, *Thermomechanical theory of martensitic phase transformations in inelastic materials*, Int. J. Solids Structures, **35**, 889–940, 1998.

10. F. D. FISCHER and G. REISNER, *A criterion for the martensitic transformation of a microregion in an elastic-plastic material*, Acta Mater., **46**, 2095–2102, 1998.

11. G. REISNER, F. D. FISCHER, Y. H. WEN and E. A. WERNER, *Interaction energy between martensitic variants*, Met. Mater. Trans., A, **30A**, 2583–2590, 1999.

12. E. GAUTIER and A. SIMON, *Transformation plasticity mechanisms for martensitic transformation of ferrous alloys*, [In:] Int. Conf. on Phase Transformations '87, G. W. LORIMER [Ed.], The Inst. of Metals, 285–287, London 1988.

13. E. GAUTIER, X. M. ZHANG and A. SIMON, *Role of internal stress state on transformation induced plasticity and transformation mechanisms during the progress of stress induced phase transformation*, [In:] Int. Conf. on Residual Stresses – ICRS 2, G. BECK, S. DENIS and A. SIMON [Eds.], Elsevier Applied Sciences, 777–783, London and New York 1989.

14. F. D. Fischer, G. Reisner, E. Werner, K. Tanaka, G. Cailletaud and T. Antretter, *A new view on transformation induced plasticity*, Int. J. Plasticity, **16**, 723–748, 2000.

15. G. Reisner, E. A. Werner and F. D. Fischer, *Micromechanical modelling of martensitic transformation in random microstructures*, Int. J. Solids & Structures, **35**, 2457–2473, 1998.